JOURNAL OF SOLID STATE CHEMISTRY 84, 280–288 (1990)

Investigation of a Time-Dependent "Nondiscrete" Component of X-Ray Scattering from Monohalocyclohexane/Thiourea Inclusion Compounds

KENNETH D. M. HARRIS*

Department of Physical Chemistry, University of Cambridge, Lensfield Road, Cambridge CB2 1EP, United Kingdom; and Davy Faraday Research Laboratory, The Royal Institution, 21 Albemarle Street, London W1X 4BS, United Kingdom

Received June 28, 1989; in revised form September 12, 1989

Single-crystal X-ray diffraction photographs of the chlorocyclohexane/thiourea and bromocyclohexane/thiourea inclusion compounds contain two types of X-ray scattering: (a) discrete diffraction maxima (rationalized as diffraction from the thiourea inclusion compound) and (b) nondiscrete conical scattering circumscribing the unscattered X-ray beam. The intensity of the nondiscrete component increases, relative to the intensity of the discrete component, as a function of X-ray exposure time. This change in the X-ray diffraction pattern has been shown to result from an X-ray-induced structural degradation of the thiourea inclusion compound single crystal in which a polycrystalline aggregate of "pure" thiourea is produced. The crystal structure of pure thiourea differs substantially from the thiourea substructure in thiourea inclusion compounds.

Introduction

We are currently investigating several aspects of crystalline organic inclusion (i.e., host–guest) systems (*1*), with emphasis on those, such as the urea and thiourea inclusion compounds, in which the host solid contains unidirectional, nonintersecting channels (tunnels). This work has been motivated primarily with a view to understanding how the structural, dynamic, and chemical properties of the included guest species can be modified upon incarceration within different host environments. Urea and thiourea inclusion compounds are of particular interest since, in some respects, they represent organic analogs of those zeolites (such as theta-1, mordenite, and zeolite L) which have unidirectional tunnel structures.

The halocyclohexane/thiourea inclusion compounds are particularly intriguing since, in many cases, the halocyclohexane molecule is compelled to exhibit uncharacteristic conformational behavior when incarcerated within the thiourea channel (*2–6*). We have previously (*7*) used single-crystal X-ray diffraction and computational methods to probe various structural aspects of chlorocyclohexane/thiourea. Although these investigations were concerned primarily with structural properties of the

* Present address: Department of Chemistry, University of St. Andrews, St. Andrews, Fife KY16 9ST, Scotland.

0022-4596/90 $3.00

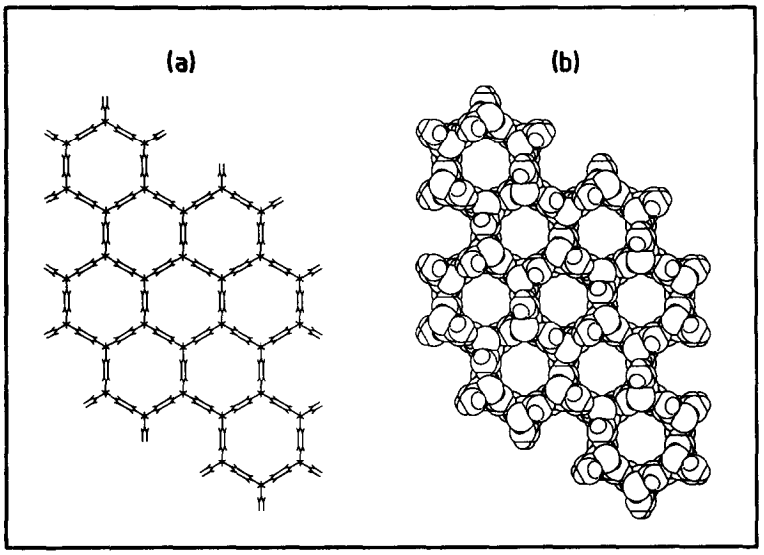

FIG. 1. Two representations, showing nine complete channels, of the host (thiourea) substructure in $C_6H_{11}Cl$/thiourea, viewed along the channel axis. The atomic radii are zero in a, whereas conventional van der Waals radii are used in b. Space group $R\bar{3}c$; a = 10.115 Å; α = 104.27°. The distance between the centers of adjacent channels is approximately 9.2 Å.

guest (chlorocyclohexane) species, it was also shown (from the X-ray diffraction data) that the host substructure is of the familiar type for thiourea inclusion compounds, containing linear, parallel, nonintersecting channels (see Fig. 1) within which the guest molecules are located. In this paper we discuss the source of a "nondiscrete" scattering component which develops, over a period of time, in single-crystal X-ray diffraction patterns of the chlorocyclohexane/thiourea ($C_6H_{11}Cl$/thiourea) and bromocyclohexane/thiourea ($C_6H_{11}Br$/thiourea) inclusion compounds.

We use the term "nondiscrete" to refer to any X-ray scattering which does *not* comprise sharp ("discrete") diffraction maxima ("Bragg reflexions"). We further subdivide nondiscrete scattering into two types: "polycrystalline" scattering and "diffuse" scattering. The former arises from a polycrystalline sample and is nondiscrete because there is a distribution (in principle, a random distribution) of crystallite orientations within such a sample. The scattering from each individual crystallite will generally (although not necessarily) comprise discrete diffraction maxima, and the spatial dispersion of the scattering from the whole sample arises because there are many different orientations of the crystallites present. True diffuse scattering, on the other hand, arises when there is a substantial degree of structural disorder (either of "static" or "dynamic" origin) within an individual crystallite and results in spatially delocalized scattering from each single crystal. (Clearly the nondiscrete scattering from a polycrystalline sample of such crystals contains both polycrystalline and diffuse contributions.) This distinction between the polycrystalline and diffuse types of nondiscrete scattering bears some analogy with the concept of line broadening in solid state NMR spectra being either "inhomogeneous" or "homogeneous" (respectively) in origin. Since we believe (see Results and Discussion) that the nondis-

crete scattering in the X-ray diffraction patterns of $C_6H_{11}Cl$/thiourea and $C_6H_{11}Br$/thiourea is of the polycrystalline type, we do *not* use the term "diffuse" when referring to this scattering. Examples of nondiscrete X-ray scattering of the diffuse type from channel-containing inclusion compounds are discussed in Refs. (*8–10*).

Experimental

$C_6H_{11}Cl$/thiourea was prepared by evaporation of solvent (at ~4°C) from a solution of $C_6H_{11}Cl$ and thiourea in methanol. The molar ratio of $C_6H_{11}Cl$ to thiourea in solution was taken in excess of the 1 : 3 ratio which is the expected stoichiometry of the inclusion compound. When sufficiently large crystals had grown, they were collected and washed with 2,2,4-trimethylpentane to remove any $C_6H_{11}Cl$ adhering to their external surfaces. A similar method was used to prepare $C_6H_{11}Br$/thiourea. Freshly prepared crystals, examined by optical microscopy, possessed the morphological characteristics (hexagonal prisms) and optical properties (uniaxial) expected for thiourea inclusion compounds.

Photographic single-crystal X-ray diffraction experiments were carried out on a Stoe Weissenberg camera (Model 3.11.2) and on a Stoe reciprocal lattice explorer (Model 3.14.0) using, in both cases, Ni-filtered Cu$K\alpha$ radiation (20 mA; 40 kV). Diffractometric single-crystal X-ray diffraction studies were performed on an Enraf-Nonius CAD4 diffractometer using graphite monochromated Mo$K\alpha$ radiation (26 mA; 52 kV).

Results and Discussion

Single-crystal X-ray diffraction oscillation photographs recorded for $C_6H_{11}Cl$/thiourea (see Fig. 2) and $C_6H_{11}Br$/thiourea typically contain two types of X-ray scat-

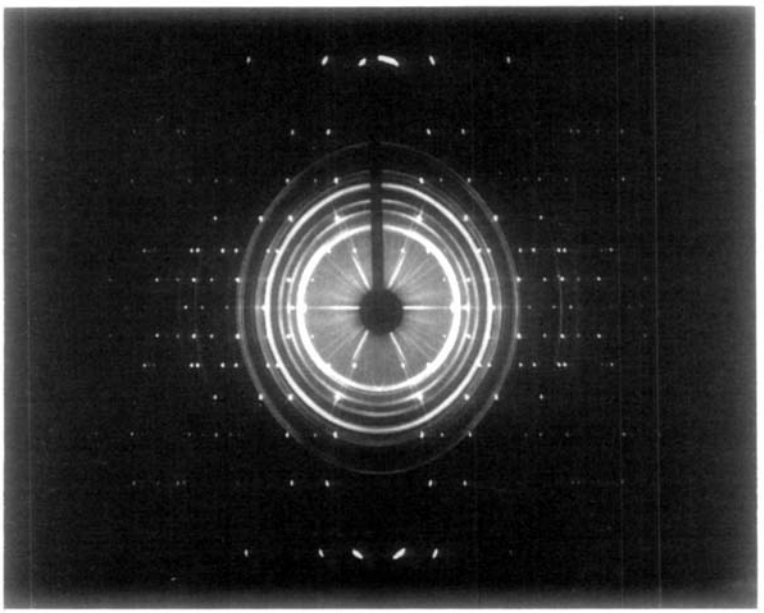

FIG. 2. X-ray diffraction oscillation photograph, recorded at room temperature, for a $C_6H_{11}Cl$/thiourea single crystal oscillating about its prism axis (i.e., the channel axis). Prior to recording this photograph, the crystal had received a total of 5 hr X-ray exposure. The X-ray exposure time while recording the photograph was 3 hr.

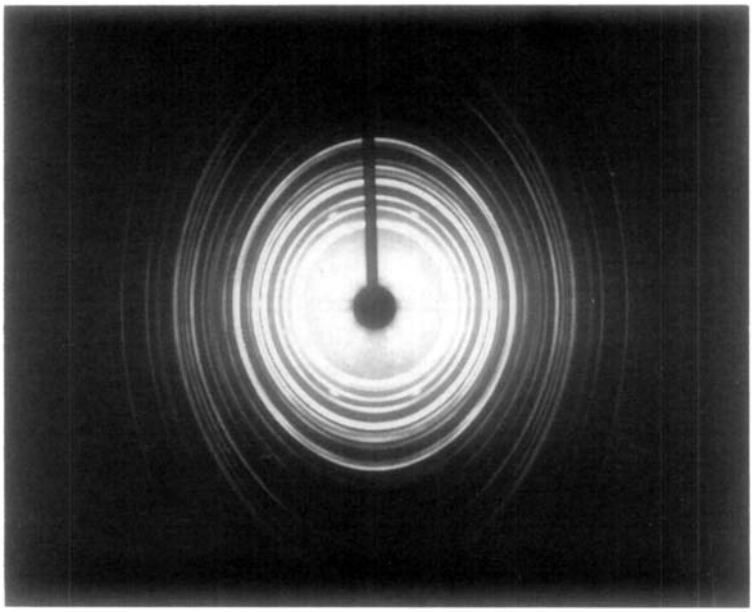

FIG. 3. X-ray diffraction oscillation photograph, recorded at room temperature, for the same $C_6H_{11}Cl$/thiourea single crystal used to obtain Fig. 2. Prior to recording this photograph, the crystal had received a total of 120 hr X-ray exposure. The X-ray exposure time while recording the photograph was 4 hr.

tering: (a) sharp, discrete spots (Bragg reflexions) which, as discussed elsewhere (*7*), are completely rationalized as diffraction from the thiourea inclusion compound and (b) a set of concentric, "pseudo-elliptical" rings (nondiscrete scattering) centered at the center of the film. The source of the nondiscrete scattering is the subject of this paper, and the following observations relate to this component of the diffraction pattern:

(A) Upon continued exposure to Cu$K\alpha$ X-radiation, the relative intensity of the nondiscrete scattering increases (relative to the intensity of the discrete reflexions) until eventually only the nondiscrete diffraction pattern remains. The growth in intensity of the nondiscrete diffraction pattern is apparently faster for $C_6H_{11}Br$/thiourea than for $C_6H_{11}Cl$/thiourea.

(B) The nondiscrete diffraction patterns for $C_6H_{11}Cl$/thiourea and $C_6H_{11}Br$/thiourea are identical.

(C) Crystals that have been subjected to prolonged X-ray exposure (Cu$K\alpha$ radiation) eventually exhibit *only* the nondiscrete diffraction pattern (Fig. 3). Such "crystals" still possess the characteristic morphology of thiourea inclusion compounds (hexagonal prisms) but, in contrast to crystals of the inclusion compound examined immediately after preparation, they do not transmit polarized light and remain extinguished for each orientation of the crystal with respect to the crossed polarizer and analyzer on the optical microscope. Furthermore, crystals which show only the nondiscrete diffraction pattern do not cleave in the normal manner but crumble to form a polycrystalline powder when an attempt is made to cut them.

Observation (A) suggests that the structural change giving rise to the nondiscrete diffraction pattern does *not* occur independently of the host substructure: i.e., it does not arise only from an alteration within the

guest substructure. Observation (C) suggests that the material, which was originally a single crystal of a thiourea inclusion compound, has become polycrystalline. This notion is consistent with the fact (discussed fully below) that the rings which constitute the nondiscrete component of the X-ray diffraction pattern are of precisely the form expected from a polycrystalline sample.

We now consider this polycrystalline scattering in more detail in order to establish the structural basis for the observations described above. X-ray scattering from a polycrystalline material occurs in cones which circumscribe the unscattered (i.e., $2\theta = 0°$) beam. On the Weissenberg camera used to record the oscillation photographs shown in Figs. 2 and 3, the film is contained within a cylindrical cassette with the cylinder axis perpendicular to the incident beam. As shown in the Appendix, conical polycrystalline scattering will intersect this film in rings which, when the film is laid flat, are described by the following equation:

$$\mathbf{Y} = \pm\sqrt{\frac{A^2 \tan^2 2\theta - A^2 \tan^2(\mathbf{X}/A)}{1 + \tan^2(\mathbf{X}/A)}} \quad \text{with } \tan^2(\mathbf{X}/A) \leq \tan^2 2\theta,$$

where A represents the radius of the cylindrical film cassette when recording the photograph and 2θ is the semi-angle of the conical scattering. $\mathbf{X}$ and $\mathbf{Y}$ specify horizontal and vertical Cartesian axes, respectively (intersecting at the center of the film), in Figs. 2 and 3.

In principle, the semi-angles of the scattering cones can be determined from the dimensions of the rings in these photographs. (In particular, when $\mathbf{Y} = 0$, $2\theta = \mathbf{X}/A$, and hence careful measurement of $\mathbf{X}$ at this position allows a straightforward determination of 2θ.) However, a more satisfactory assessment of 2θ values is achieved by recording the oscillation photograph with a flat film perpendicular to the incident beam, since the film in such an arrangement intersects the conical polycrystalline scattering in circular rings. The required geometry (Fig. 4) is established on the combined de Jong-Bouman/precession camera (Stoe reciprocal lattice explorer) by: (a) setting the inclination angle (conventionally denoted μ) to zero (so that the incident beam is perpendicular to the crystal rotation axis), (b) mounting the planar film in the (fixed) position conventionally used for precession photography, and (c) rotating the crystal as for a de Jong-Bouman photograph. Moreover, the crystal-to-film distance (M in Fig. 4) can be altered with this apparatus, allowing circular sections to be taken at different positions through the conical scattering and therefore allowing an independent determination of the same set of cone semi-angles from different photographs. The semi-angle of the conical scattering is the diffraction angle 2θ and the set of d-spacings giving rise to the polycrystalline diffraction pattern can be deduced directly from Bragg's Law.

The d-spacings determined via this method are presented in Table I, together with the d-spacings calculated for the known crystal structure of "pure" thiourea (*11*). (Note that this crystal structure is *not* the same as the thiourea substructure in thiourea inclusion compounds: in particular, it does *not* contain "empty" channels.) From the close agreement, in Table I, between the sets of d-spacings in columns 1 and 2 compared with those in column 3, the nondiscrete diffraction pattern clearly arises from polycrystalline pure thiourea. Evidently, structural degradation of the inclusion compound (i.e., collapse of the thiourea channel structure) occurs over a period of time, leading to recrystallization as polycrystalline thiourea.

We now discuss the origin of this structural transformation in more detail. After preparation, the thiourea inclusion compounds were stored at $-16°C$ until required

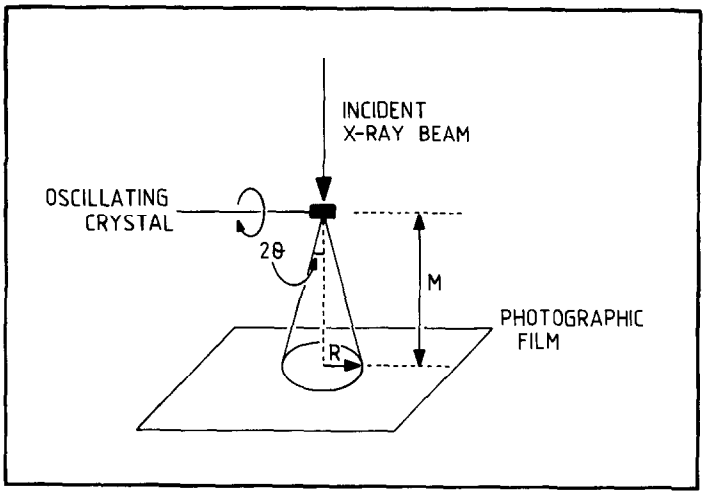

FIG. 4. Geometrical information relating to the technique used to investigate the "nondiscrete" scattering which develops in the X-ray diffraction patterns of $C_6H_{11}Cl$/thiourea and $C_6H_{11}Br$/thiourea. Note: (i) M is the crystal-to-film distance, (ii) R is the radius of the circular ring produced on the film by the scattering cone with semi-angle 2θ. Clearly, $2\theta = \tan^{-1}(R/M)$, and from Bragg's Law,

$$d = \frac{\lambda}{2 \sin((\frac{1}{2}) \tan^{-1}(R/M))}.$$

for experimental use, and the change in the diffraction pattern during room temperature (~23°C) X-ray diffraction experiments probably results either from thermally induced or from X-ray induced degradation. Typically, no discrete scattering remains in the X-ray diffraction patterns of $C_6H_{11}Cl$/thiourea single crystals which have received about 100 hr of Cu$K\alpha$ X-ray irradiation at room temperature (see Fig. 3). Crystals maintained at room temperature for this length of time *before* exposure to Cu$K\alpha$ X-radiation show predominantly discrete scattering and only weak polycrystalline scattering. These observations suggest that the structural change is primarily X-ray induced. (Since we use X-ray diffraction to assess the structural characteristics of the system, it is not possible for us to monitor the structural degradation of the crystal without it having received some amount of X-ray irradiation. We cannot therefore assess readily whether the production of the polycrystalline phase can *also* be brought about thermally: it is clear, however, that thermal degradation, if it occurs, must be appreciably slower than the X-ray induced structural change.)

Further support for these conclusions comes from considering the relative rates with which the discrete scattering from the inclusion compound single crystal is replaced by the polycrystalline scattering from pure thiourea when using different incident X-ray wavelengths. In our diffractometric measurement of the discrete X-ray reflexions from $C_6H_{11}Cl$/thiourea using Mo$K\alpha$ radiation (*7*), no appreciable diminution in the intensities of "control reflexions" occurred during the entire data collection. The duration of this experiment was comparable to the time required for a substantial decrease in the relative intensities of discrete reflexions during photographic X-ray diffraction experiments (using Cu$K\alpha$ radiation) at the same temperature (room temperature). Since the crystals used in these studies were at room tem-

TABLE I

COMPARISON BETWEEN (A) *d*-SPACINGS DETERMINED (VIA THE METHOD OUTLINED IN FIG. 4) FOR THE "POLYCRYSTALLINE" RINGS IN THE X-RAY DIFFRACTION PATTERN OF $C_6H_{11}Cl$/THIOUREA; AND (B) *d*-SPACINGS CALCULATED FOR THE REPORTED CRYSTAL STRUCTURE OF "PURE" THIOUREA (*11*)

Measured *d*-spacings		Calculated *d*-spacings for pure thiourea *d* (Å)
M = 35 mm *d* (Å)	M = 60 mm *d* (Å)	
4.56	4.60	4.64
4.44	4.43	4.48
4.25	4.28	4.27
		3.97
3.83	3.80	3.83
3.48	3.48	3.49
		3.15
3.10	3.08	3.09
2.94	2.94	2.95
2.85	2.84	2.85
2.74	2.74	2.76
		2.60
2.53	2.53	2.53
2.45	2.44	2.48
		2.40
2.31	2.30	2.32
		2.28
		2.24
		2.22
2.16	2.15	2.17
		2.13
2.10	2.10	2.11
2.02	2.02	2.04

Note. Space group *Pnma*; a = 7.655 Å; b = 8.537 Å; c = 5.520 Å. *d*-spacings have been measured only for the more intense rings in the X-ray diffraction photographs and the blank entries in columns 1 and 2 presumably represent rings which have not been measured because they have a low scattering intensity. Measured *d*-spacings have been determined independently from photographs recorded with crystal-to-film distances M = 35 mm and M = 60 mm (M defined in Fig. 4). The list of calculated *d*-spacings does *not* include *d*-spacings which correspond to systematically absent reflexions.

perature for comparable lengths of time, it is clear that the primary cause of the structural degradation is *not* a thermal effect. Moreover, the differing behavior in the diffractometric (Mo$K\alpha$ radiation) and photographic (Cu$K\alpha$ radiation) X-ray diffraction studies is consistent with the structural change being X-ray induced: X-ray damage of organic materials is generally more pronounced for longer wavelength radiation (Cu$K\alpha$), presumably because X-ray absorption coefficients increase as a function of increasing wavelength.

It is well known, both from experimental studies (*12*) and from computer simulation (*9*, *13*), that the "empty" urea channel structure (obtained by removing the guest species from a urea inclusion compound) is unstable and recrystallizes to the more compact crystal structure of pure urea. It is likely that the empty thiourea channel will also collapse under similar circumstances. One possible explanation for the structural change in our experiments is that X-ray induced decomposition of the included halocyclohexane molecule leads to fragmentation products which are able to escape from the thiourea channel. This would produce local regions of unoccupied channel which should then collapse spontane-

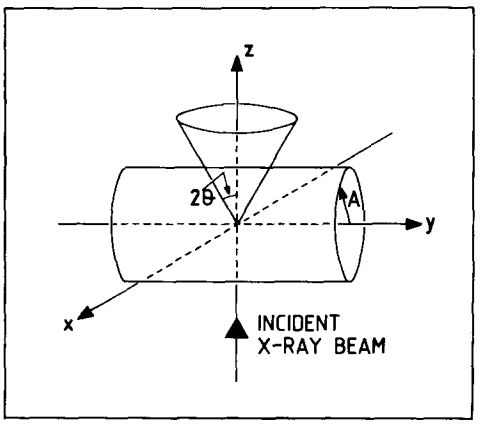

FIG. 5. Schematic representation of the cylindrical film (radius A) on a Weissenberg camera and the conical X-ray scattering (semi-angle 2θ) arising from a polycrystalline sample located at the origin. The incident X-ray beam is directed in the positive direction along the z-axis toward the origin.

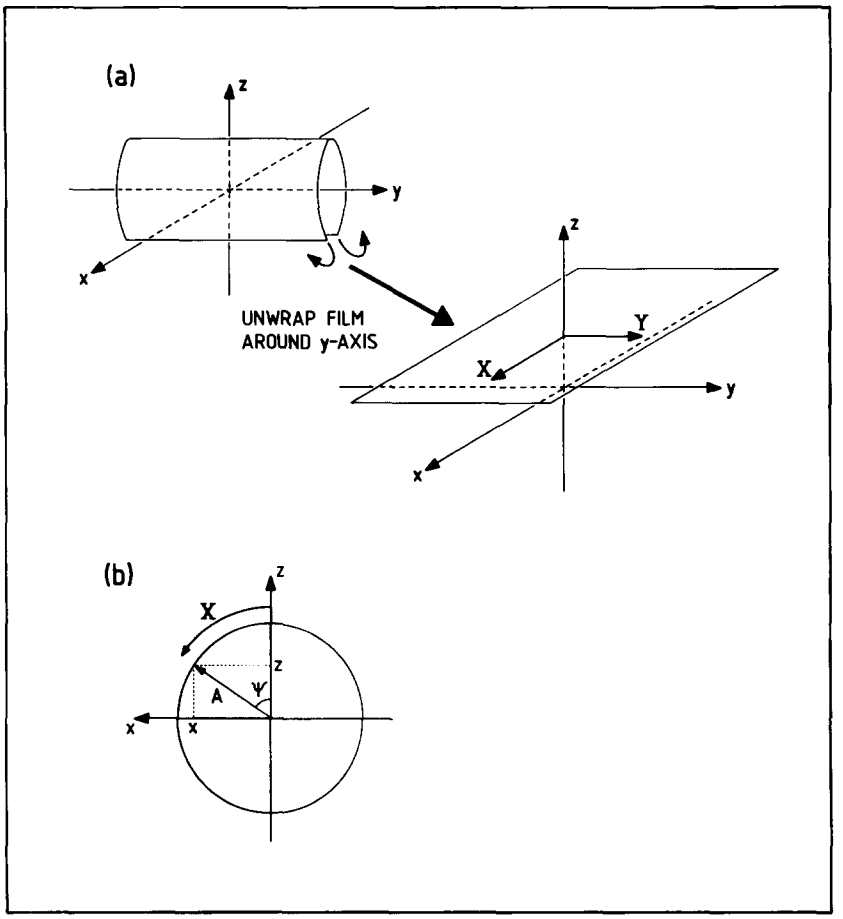

FIG. 6. Definition of the relationship between the coordinate systems (x,y,z) and $(\mathbf{X},\mathbf{Y})$ discussed in the text. Diagram b shows the relationship (viewed along y) between (x,y,z) and $(\mathbf{X},\mathbf{Y})$ before unwrapping the film.

ously and recrystallize as a polycrystalline aggregate of pure thiourea. It is notable that this polycrystalline aggregate retains the outward appearance (i.e., hexagonal prismatic shape) of the parent thiourea inclusion compound single crystal.

Finally, the fact (see observation (B) above) that the discrete diffraction pattern from $C_6H_{11}Br$/thiourea disappears extremely rapidly as a function of X-ray exposure time (both with Cu$K\alpha$ and Mo$K\alpha$ radiations) has precluded the possibility of carrying out a full crystal structure determination of this material. Several X-ray diffraction studies of thiourea inclusion compounds, containing a diverse range of guest species, have been reported previously, but in none of these cases are we aware that significant degradation of the channel structure was observed. It is not certain why the monohalocyclohexane/thiourea systems discussed here should be particularly problematic in this respect.

Appendix

The equations for the intersecting cone and cylinder shown in Fig. 5 are:

$$\text{Cone: } x^2 + y^2 = z^2 \tan^2 2\theta \quad (1)$$

$$\text{Cylinder: } x^2 + z^2 = A^2. \quad (2)$$

By eliminating x and z, respectively, from Eqs. (1) and (2) and rearranging, we obtain:

$$z^2 = \frac{A^2 + y^2}{1 + \tan^2 2\theta} \quad (3)$$

$$x^2 = \frac{A^2 \tan^2 2\theta - y^2}{1 + \tan^2 2\theta}. \quad (4)$$

Eqs. (3) and (4) define the intersection between the cone and cylinder shown in Fig. 5, and specify the equation for the ring produced on the film by the scattering cone with semi-angle 2θ when the film is contained within the cylindrical film cassette. Now consider removing the film from the cassette by unwrapping it around the y-axis so that the film, when flat, lies parallel to the xy-plane (Fig. 6a). The relationship between the new coordinate system (**X**,**Y**) relating to the flat film (note that **X** is horizontal and **Y** is vertical in Figs. 2 and 3) and the old coordinate system (x,y,z) is established from Fig. 6:

$$\Psi = \mathbf{X}/A \;\; ; \;\; \tan \Psi = x/z$$

$$\Rightarrow \mathbf{X} = A \tan^{-1}(x/z) \quad (5)$$

$$\mathbf{Y} = y. \quad (6)$$

Hence, from Eq. (5),

$$\frac{x^2}{z^2} = \tan^2(\mathbf{X}/A). \quad (7)$$

Taking x^2 and z^2 from Eqs. (4) and (3), and using Eqs. (6) and (7), it follows that:

$$\mathbf{Y} = \pm\sqrt{\frac{A^2 \tan^2 2\theta - A^2 \tan^2(\mathbf{X}/A)}{1 + \tan^2(\mathbf{X}/A)}}.$$

Acknowledgments

I am indebted to Professor J. M. Thomas, FRS (The Royal Institution) for many stimulating discussions and to British Petroleum for financial support in the form of a BP Research Studentship.

References

1. J. M. Thomas and K. D. M. Harris, *in* "Organic Solid State Chemistry" (G. R. Desiraju, Ed.), Chapt. 6, Elsevier, Amsterdam/New York (1987).
2. M. Nishikawa, *Chem. Pharm. Bull.* **11,** 977 (1963).
3. K. Fukushima, *J. Mol. Struct.* **34,** 67 (1976).
4. A. Allen, V. Fawcett and D. A. Long, *J. Raman Spec.* **4,** 285 (1976).
5. K. Fukushima and K. Sugiura, *J. Mol. Struct.* **41,** 41 (1977).
6. J. E. Gustavsen, P. Klaeboe and H. Kvila, *Acta Chem. Scand.* **A32,** 25 (1978).
7. K. D. M. Harris and J. M. Thomas, *J. Chem. Soc. Faraday Trans.*, in press.
8. M. D. Hollingsworth, K. D. M. Harris, W. Jones, and J. M. Thomas, *J. Inclusion Phenomena* **5,** 273 (1987).
9. K. D. M. Harris, PhD Thesis, Univ. of Cambridge (1988).
10. K. D. M. Harris and J. M. Thomas, in preparation.
11. M. R. Truter, *Acta Crystallogr.* **22,** 556 (1967).
12. H. G. McAdie, *Canad. J. Chem.* **40,** 2195 (1962).
13. K. D. M. Harris, S. Yashonath, and J. M. Thomas, in preparation.